RAA 2020 Vol. **20** No. **9**, 155(9pp) doi: 10.1088/1674–4527/20/9/155

http://www.raa-journal.org *http://iopscience.iop.org/raa*

Research in Astronomy and Astrophysics

AstroSat observation of the Be/X-ray binary Pulsar 3A 0726–260 (4U 0728–25)

Jayashree Roy[1,2], Prahlad C. Agrawal[1], Baibhav Singari[3] and Ranjeev Misra[2]

[1] UM-DAE Centre for Excellence in Basic Sciences, University of Mumbai, Vidyanagari Campus, Mumbai, 400098, Maharashtra, India

[2] Inter-University Center for Astronomy and Astrophysics, Post Bag 4, Pune, 411007, Maharashtra, India; *jayashree@iucaa.in*

[3] School of Physical Sciences, National Institute of Science Education and Research Bhubaneswar, Khurda, 752050, Odisha, India

Received 2020 January 22; accepted 2020 April 19

Abstract Results on timing and spectral properties of the Be/X-ray binary pulsar 3A 0726–260 (4U 0728–25) are presented. The binary was observed on 2016 May 6–7 with the Large Area X-ray Proportional Counter (LAXPC) and Soft X-ray Telescope (SXT) instruments onboard the AstroSat satellite. During this observation, the source was in non-flaring persistent state at a flux level of $\sim 8.6 \pm 0.3 \times 10^{-11}$ erg cm^{-2} s^{-1} in 0.4–20 keV. Strong X-ray pulsations with a period of 103.144$\pm$0.001 s are detected in 0.3–7 keV with the SXT and in 3–40 keV with the LAXPC. The pulse profile is energy dependent, and there is an indication that the pulse shape changes from a broad single pulse to a double pulse at higher energy. At energies above 20 keV, we report the first time detection of pulsation period 103.145$\pm$0.001 s and the double peaked pulse profile from the source. The energy spectrum of the source is derived from the combined analysis of the SXT and LAXPC spectral data in 0.4–20 keV. The best spectral fit is obtained by a power law model with a photon index (1.7$\pm$0.03) with high energy spectral cut-off at 12.9 $\pm$ 0.7 keV. A broad iron line at $\sim$ 6.3 keV is detected in the energy spectrum. We briefly discuss the implications of these results.

Key words: Be/X-ray binary, pulsar, 4U 0728–25

1 INTRODUCTION

The X-ray source 3A 0726–260 (also known as X 0726-260 and 4U 0728-25) is one of the least studied X-ray binary pulsars. This source was first reported in the Fourth Uhuru catalog (Forman et al. 1978). Further, X-ray detections were published by results from Ariel V (Warwick et al. 1981) and HEAO-1 (Wood et al. 1984). From the Scanning Modulation Collimator experiment on HEAO-1, Steiner et al. (1984) identified the X-ray source with a B0 type star at a distance of 4.6–6 kpc. The optical spectrum of the star showed a broad Hα line (13 Å FWHM) in emission and Hβ line in absorption, suggesting it to be a Be binary (Steiner et al. 1984). Corbet & Mason (1984) found both Hα (5.5 Å) and weak Hβ (0.4 Å) emission lines in the spectra of the optical counterpart and revised its spectral type as B0Ve and distance as $\sim$ 4.6$\pm$ 1.6 kpc. Negueruela et al. (1996) studied the optical spectra and performed photometry in the optical and infrared region of the Be star and classified it as an O8-9Ve type star at a distance of $\sim$ 6.1$\pm$0.3 kpc. Despite being a persistent X-ray emitter at luminosity level of $\sim 10^{35}$ erg s^{-1} during non-flaring states, 3A 0726–260 is one of the least studied X-ray binaries. The only reported X-ray study of this binary is by Corbet & Peele (1997), who analyzed its 1996 observations by the All Sky Monitor (ASM) and Proportional Counter Array (PCA) instruments onboard the Rossi X-ray Timing Explorer (RXTE) satellite. From the PCA light curves, they discovered that this binary has an X-ray pulsar with a spin period of 103.2$\pm$0.1 s. They also inferred from the ASM light curve the orbital period of the binary $\sim$ 34.5 days, and its harmonic at 17.5 days. The orbital period has been refined to be 34.5446$\pm$0.0153 days by Nakajima et al. (2016), considering MAXI/GSC observations. Moreover, the improved value of the orbital period to 34.548$\pm$0.010 days was reported by Nakajima et al. (2016) by using Swift-BAT data. Corbet & Peele (1997) also studied the energy spectrum of this binary in 2–20 keV from the RXTA-PCA data and found that it is described well by an absorbed power law model. They derived a photon index of 1.58±0.03 and a hydrogen column density of 0.3×10^{22} cm^2. Estimated unabsorbed 2–20 keV X-ray flux with this model is 6.9×10^{-11} erg cm^{-2} s^{-1}. AstroSat revisited this source in 2016 May 6–7 ∼ 20 years after its RXTE observations. We present results from broadband (0.3–40 keV) study of the source using data from AstroSat observations with the Soft X-ray Telescope (SXT) and the Large Area X-ray Proportional Counter (LAXPC) detectors. Results on the spin period, energy dependent pulse profile and pulsed fraction of the source are presented in this paper. We have also analyzed the broadband spectrum of the source in a 0.4–20 keV X-ray band and report the detection of a broad iron line at 6.3 keV in its spectrum. The paper is structured as follows: introduction in Section 1 is followed by a description of observation and data reduction in Section 2. In Section 3, we present results from the timing and spectral analysis. Details of the timing analysis, e.g. power density spectrum (PDS) of the pulsar, spin period, pulse profiles and pulse fraction, are reported in subsection 3.1. In Section 4, we present results of the spectral analysis, as well as their implication on the source model.

2 OBSERVATIONS AND DATA REDUCTION

The binary 3A 0726–260 was observed with the SXT and LAXPC instruments onboard the AstroSat satellite on 2016 May 6 from 19:59:47.2 hh:mm:ss UTC to 2016 May 7 22:54:29.2 hh:mm:ss UTC, comprising 14 orbits, for a total duration of ∼ 91 ks. A description of the AstroSat satellite and its instruments is provided in Agrawal (2006) and Singh et al. (2014).

The LAXPC instrument consists of three identical collimated detectors (LAXPC 10, LAXPC 20 and LAXPC 30) covering the energy range 3–80 keV, and having a five anode layer geometry with 15 cm deep X-ray detection volume providing an effective area of about 6000 cm^{-2} at 10 keV. LAXPCs are filled with a xenon-methane (90%:10%) mixture at 1520 torr and have a field of view of $0.9^\circ\times0.9^\circ$. Every valid photon event detected in the LAXPC detectors is time tagged to an accuracy of 10 µs. Detailed description of the characteristics of the LAXPC instrument can be found in Yadav et al. (2016), Agrawal et al. (2017) and Roy et al. (2016), and calibration details in Antia et al. (2017).

Level 1 data are converted to Level 2 data using the LAXPC pipeline laxpcsoft[1] version 2018 May 19. Level-2 data contain (i) light curve in broad band counting mode (modeBB) and (ii) event mode data (modeEA) with information about the arrival time, pulse height and the layer of origin for each detected X-ray; (iii) housekeeping data and parameter files are stored in an mkf file. The laxpc pipeline removes the overlapping data between consecutive orbits. Good time intervals were generated by filtering out Earth occultation and passages of South Atlantic Anomaly (SAA) regions. This pipeline software has individual routines to extract light curves and background light curves. We have utilized event mode data (ModeEA) for our analysis. This code generates a background model that is based on the observations of source-free sky regions. For our work, we have used data from only LAXPC 10 and LAXPC 20 units, as the gas gain of LAXPC 30 was not stable due to gas leakage (Antia et al. 2017). The LAXPC source and background light curves are generated by the 'laxpc_make_lightcurve' and 'laxpc_make_backlightcurve' tasks of LAXPCsoftware respectively. We generated energy dependent light curves in the energy bands 3–5 keV, 5–8 keV, 8–20 keV and overall 3–20 keV considering data only from the top layer of LAXPC, as most incident photons (∼ 90%) of $<$ 20 keV energy are absorbed in the top layer comprising Anode 1 and Anode 2. Further, the light curves in 20–40 keV and 3–40 keV are generated from both LAXPCs 10 and 20, from the top layer only, as including other layers increased the background counts which dominated the source photons. For the timing analysis, combined data from the two LAXPCs were used. For the spectral analysis, we considered data obtained only from LAXPC 10 and LAXPC 20 separately with 512 and 256 channel binning as suggested by (Antia et al. 2017) and employed the single routine LAXPC pipeline laxpcsoftv3.0.

SXT onboard AstroSat is a soft X-ray telescope sensitive in the 0.3–8 keV range. The effective area of SXT is ∼ 90 cm^2 at 1.5 keV. A detailed description of the SXT instrument can be found in Singh et al. (2016, 2017). The SXT observations of 3A 0726–260 were in the photon counting mode. Full frame readout time resolution of the detector is ∼ 2.4 s in SXT photon counting mode. The SXT level 1 data from 14 orbits were processed implementing SXTPIPELINE version AS1SXTLevel2-1.4b[2] released on 2019 January 3, to generate level 2 data for each orbit. Level 2 SXT data are filtered out from contamination by the charged particles from excursions through the SAA region and Earth occultation. All the events with grade $>$ 12 were removed in the level 2 data. Merged event files from all the individual orbits were produced using python script sxt_gti_corr_evt_merger_v05.py[3]. A circular region with 8 arcmin radius centered on the source and another circular region of 8 arcmin radius away from the source location were used to extract the light curves and spectra for the

[1] http://astrosat-ssc.iucaa.in/?q=laxpcData

[2] http://www.tifr.res.in/~astrosat_sxt/sxtpipeline.html

[3] http://www.tifr.res.in/~astrosat_sxt/dataanalysis.html

source and background, respectively. The light curve and spectrum were generated using XSELECT under HEASoft (v 6.25).

A barycentric correction was applied on the light curves to incorporate the effect of Earth and satellite motion relative to the barycenter of the solar system. For the timing analysis of LAXPC, event files are barycenter corrected using AstroSat's barycentric correction tool as1bary[4]. We applied ftool earth2sun[5] for barycenter correction of the SXT light curve. The data were analyzed using HEASOFT 6.25[6]. HEASOFT consists of (mainly) FTOOLS for general data extraction and analysis, XRONOS (Stella & Angelini 1992) for timing analysis and the XSPEC package (Arnaud 1996) for spectral analysis. Table 1 lists details on count rates of 3A 0726–260 observed from the SXT and LAXPC detectors.

3 DATA ANALYSIS

3.1 Timing Analysis

A one day binned MAXI light curve of the source from MJD 55066.5 to MJD 58457.5, in 2-20 keV along with the AstroSat observation on MJD 57514.83 indicated with a thick black vertical line, is marked in Figure 1. As seen from the MAXI[7] light curve, the AstroSat observation was made when the source was in a quiescent state.

Source and background light curves were extracted from the data of 14 orbits in 3–20 keV with a time resolution of 1 s for the LAXPCs, and a time resolution of 2.3775 s for the SXT in 0.3–7 keV. The X-ray light curves with 10 s binning are presented in Figure 2 for the SXT, LAXPC 10, LAXPC 20 and combined rates of the two LAXPCs. Estimated background rates are also presented in red in the same panels. The systematic error of 2% is added to the background light curve as suggested by the background light curve analysis task 'laxpc_make_backlightcurve' in LAXPCsoftware (Format A)[8].

PDS of the source is generated using the 1 s binned, combined light curves of LAXPC 10 and LAXPC 20 employing ftool "powspec" in HEASOFT. The light curve was divided into stretches of 4096 bins per interval. The PDSs from all the segments were averaged to produce the final PDS for the observation. Poissonian noise was subtracted from the PDS, and it was normalized such that its integral gives the squared root mean square (rms) fractional variability normalized to units of (rms/mean)^2 Hz^{-1}. PDS generated from 0.2 mHz to 0.5 Hz manifested a very strong peak pertaining to the spin period of the source at $9.7^{+0.03}_{0.03}$ mHz and two harmonics at $0.2^{+0.01}_{-0.01}$ mHz and $0.3^{+0.01}_{-0.01}$ mHz as seen in Figure 3. An estimate of the pulsation period with better precision is achieved by applying the standard χ^2 maximization technique with the ftools task "efsearch".

The pulsation period is searched around the approximate period 102.89 s, as observed in the PDS generated from the combined LAXPC light curve. The 1 s binned light curve is folded with 8192 different periods around the approximate period with 1 ms resolution and 16 phase bin per period. The distribution between the maximum χ^2 and the pulsar period displays a Gaussian profile indicating the detected pulsation period. This pulsation peak was fit with a Gaussian function to estimate the pulse period. The error on the Gaussian center is the error in the observed pulsation period. Following the same methodology for the estimation of the pulsation period, as done with the LAXPC light curve, the pulse period from the SXT data is estimated from the 2.3775 s binned light curve of SXT using 2048 different periods around the approximate period. We were unable to execute 8192 different period searches around the approximate period as SXT's bin time is 2.3775 s, unlike 1 s binning of LAXPC light curves. The pulsation period value is highlighted in different energy bands for SXT and LAXPC in the left panels and right panels of Figure 4 respectively. The best estimated pulse periods from all the observations are tabulated in Table 1.

Pulse profiles in different energy bands were generated by folding the light curve using the ftool "efold" over the exact pulsation period 103.144 s obtained by the standard χ^2 maximization technique of LAXPC light curve. The pulse profiles were generated with 16 phase bins per period. The pulse profiles in 0.3–2 keV and 2–7 keV for background subtracted SXT light curves are shown in the left panels of Figure 5. The pulse profiles in 3–5 keV, 5–8 keV, 8–20 keV and 20–40 keV background subtracted light curves of LAXPC are displayed in the right panels of Figure 5. The pulse profile in 0.3–2 keV and 2–7 keV from the SXT, and 3–5 keV and 5–8 keV from the LAXPCs manifest similar shape with a broad pulse. The pulse shape in 8–20 keV and 20–40 keV appears different with a double hump pulse profile. This suggests that the pulse shape is energy dependent. The pulse fraction of pulse profiles is calculated from the relation ($F_{\rm max}$-$F_{\rm min}$)/($F_{\rm max}$+$F_{\rm min}$), where $F_{\rm max}$ and $F_{\rm min}$ are the maximum and minimum values of the observed photon flux respectively (Nespoli & Reig 2011). It is noticed that the pulse fraction in 3–20 keV inferred from the LAXPCs is constant at about 15%. The 2–7 keV pulse fraction from

4 http://astrosat-ssc.iucaa.in/?q=data_and_analysis
5 https://heasarc.gsfc.nasa.gov/ftools/fhelp/earth2sun.txt
6 https://heasarc.gsfc.nasa.gov/lheasoft/download.html
7 http://maxi.riken.jp/top/slist.html
8 http://astrosat-ssc.iucaa.in/?q=laxpcData

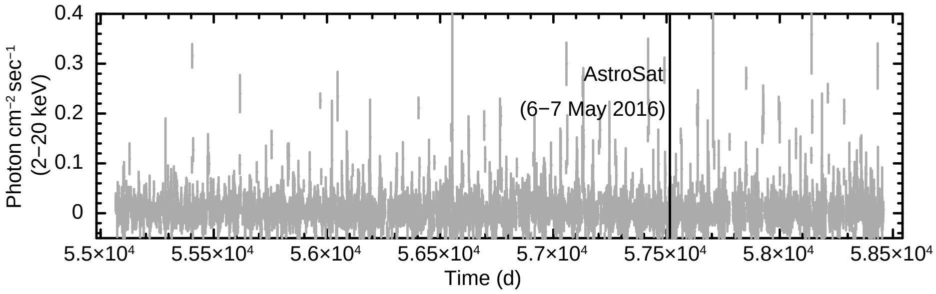

Fig. 1 MAXI one day binned light curve in 2–20 keV energy band from MJD 55066.5 to MJD 58457.5 of the source 3A 0726–260 is depicted in this plot. AstroSat observation on MJD 57514.83–57515.95 (2016 May 6–7) is indicated with a thick black vertical line.

Table 1 SXT and LAXPC Average Count Rates in Different Energy Bands for 3A 0726–260 and Background

Observations	Energy Range (keV)	Average Count (counts s^{-1})	Pulsation Period (s)	Pulsed Fraction (%)
		SXT		
Source (+Background)	0.3-2	0.13±0.003	103.144±0.001	
	2-7	0.11±0.003	103.141±0.002	
Background	0.3-2	0.02±0.001	-	
	2-7	0.01±0.001	-	
Source (-Background)	0.3-2	0.11±0.004	-	42.2±10.0
	2-7	0.10±0.003	-	26.8±10.0
		LAXPC		
Source (+Background)	3–5	16.6±0.02	103.147±0.001	
	5–8	18.0±0.02	103.144±0.001	
	8–20	35.0±0.03	103.144±0.001	
	3–20	69.3±0.04	103.144±0.001	
	20–40	33.0±0.03	103.145±0.001	
Background	3–5	11.0±0.2	-	
	5–8	11.3±0.2	-	
	8–20	26.0±0.5	-	
	3–20	51.2±1.0	-	
	20–40	31.2±0.6	-	
Source (-Background)	3-5	5.6±0.2	-	16.0±1.1
	5–8	6.7±0.2	-	14.8±1.0
	8–20	8.7±0.5	-	14.2±1.0
	3–20	18.1±1.0	-	13.4±0.7
	20–40	1.5±0.6	-	23.0±6.0

The error on the LAXPC background count rate is 2% systematic errors. Pulsation period and pulsed fraction in different energy intervals of SXT and LAXPC are presented in this table.

SXT is 26.0±10, and considering the large error, it is also consistent with a mean pulse fraction of 15%. The pulse fraction in 0.3–2 keV seems to suggest a larger value, but given the large uncertainty associated with it, no definite conclusion can be drawn about its energy dependence.

3.2 Spectral Analysis

We have performed a combined broadband spectral analysis of SXT in 0.4–7 keV and LAXPC units 10 and 20 in 3–20 keV. The LAXPC spectrum is extracted from the top layer (Anodes 1 and 2) data of the merged 14 LAXPC orbits. The spectrum is extracted from the top layer to optimize the inclusion of X-ray photons and reduce the background. The LAXPC software[9] used for spectral studies has a single routine to extract the source spectra, background spectra and response matrix files. The script 'laxpcl1.f' provided with the software processes the level-1 orbit data to generate the level-2 standard products like the event file, spectrum for source and background. To correct for the drift in the gain of the detectors with time, we have used the script 'backshift.f' provided with the software. This code generates a background model which is based on the observations of source-free sky regions. The background LAXPC data closest to gain are chosen.

A gain correction is applied to the SXT spectra by freezing gain slope to value 1[10] and the gain offset was allowed to vary with the fit as suggested by the SXT in-

[9] http://astrosat-ssc.iucaa.in/?q=laxpcData

[10] http://astrosat-ssc.iucaa.in/uploads/sxt/readme_sxt_arf_data_analysis.txt, https://www.tifr.res.in/~astrosat_sxt/instrument.html

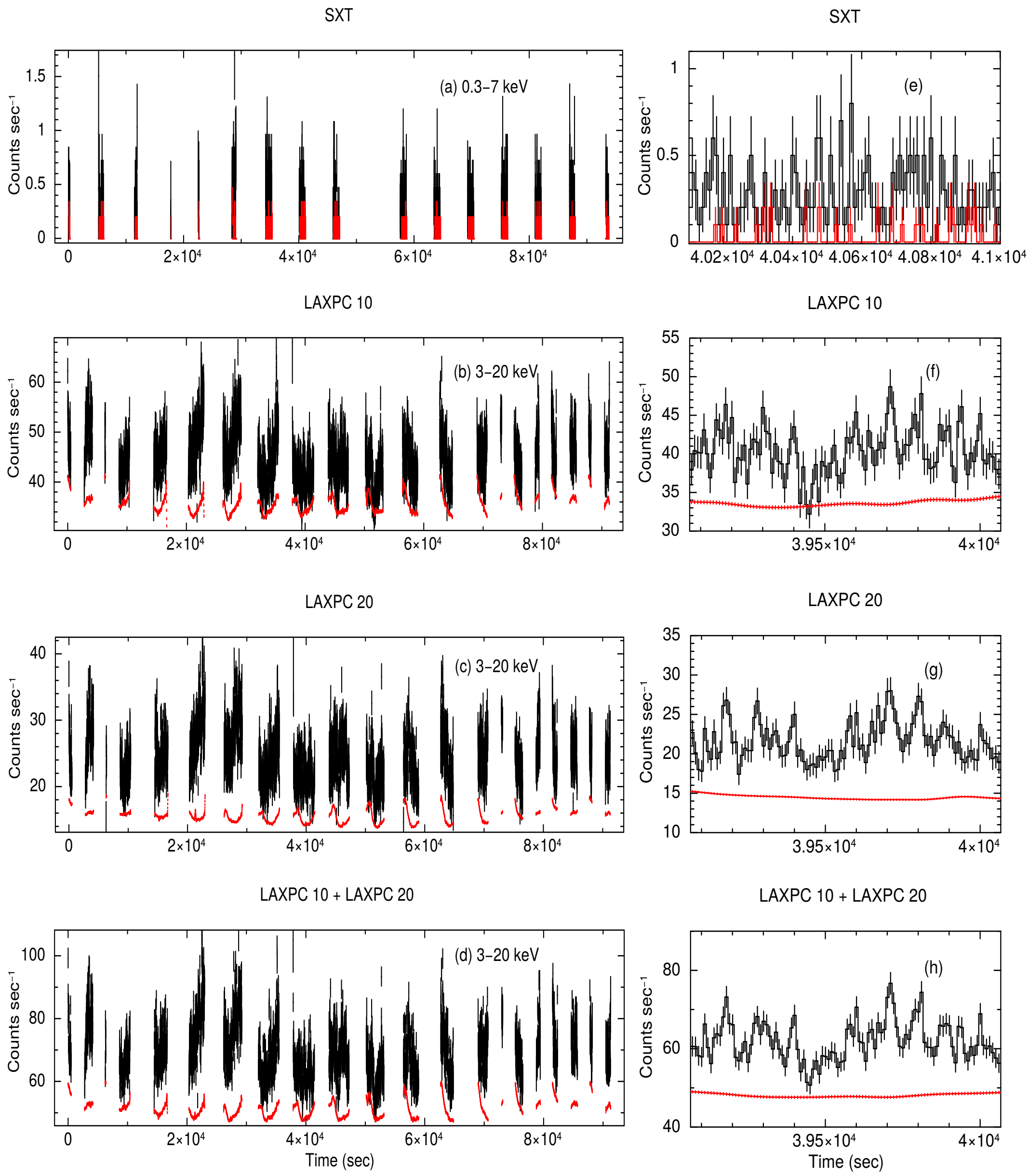

Fig. 2 Top panel (a) displays the SXT light curve of 3A 0726–260 in the 0.3–7 keV energy range. Panel (b) depicts the 3–20 keV LAXPC 10 light curve and panel (c) highlights the LAXPC 20 light curve. The bottom panel (d) provides the combined LAXPC 10 and LAXPC 20 light curves. All the barycenter corrected light curves shown in this plot are in 10 s bins. Estimated background rates for the detector are presented in the same panel in red. The gaps in the light curve are due to the passage of the satellite through the SAA regions. Right panels (e), (f), (g) and (h) show the zoomed in 10 s binned light curve of the left panels of SXT, LAXPC 10, LAXPC 20 and combined LAXPC 10 and 20 light curves respectively. These zoomed in light curves showcase $\sim$ 103 s periodicity of the source. The LAXPC error on the background count rate (presented in red) is 2% systematic errors.

strument team. We obtained an offset of -0.12 ± 0.02. The SXT spectrum of the pulsar was fitted with an absorbed powerlaw model that included an interstellar absorption TBabs (Wilms et al. 2000) and powerlaw[11] listed in XSPEC. The value of column density is fixed at the N_H value obtained from the SXT 0.4–7 keV energy spectrum, N_H=0.75×10^{22} cm^{-2} for the combined SXT and LAXPC spectral fitting. The combined spectrum gave a poor fit with χ^2/dof value of 478/171 with 2% systematics used for spectral fitting.

$$f(E) = KE^{-\Gamma} \times \begin{cases} 1 & (E \leq E_c) \\ \exp(E_c - E)/E_f & (E > E_c), \end{cases} \quad (1)$$

where K is normalization factor (photon keV^{-1}cm^{-2}s^{-1} at 1 keV), Γ is photon index of powerlaw, E is the photon

[11] https://heasarc.gsfc.nasa.gov/xanadu/xspec/manual/node211.html

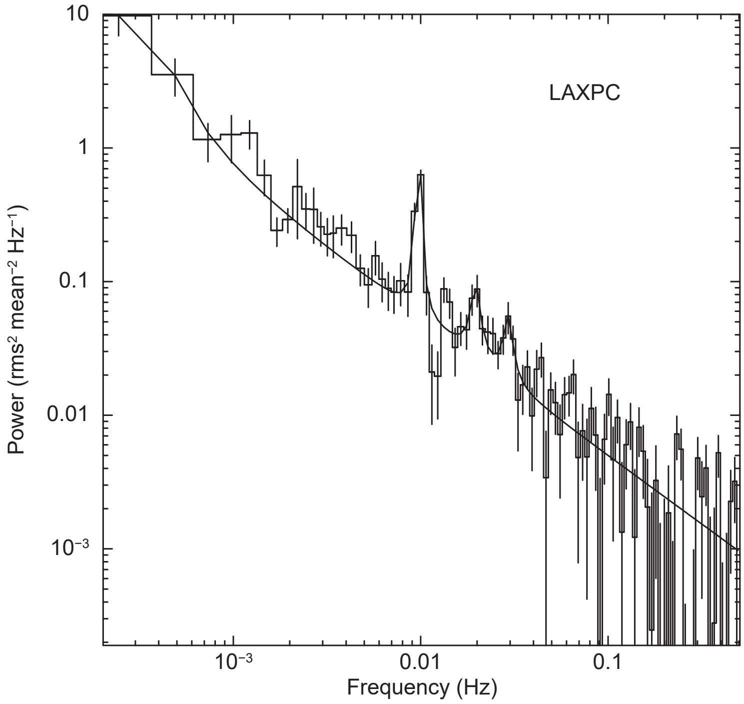

Fig. 3 The PDS of 3A 0726–260, generated using the combined LAXPC 10 and LAXPC 20 data from 1 s binned barycenter corrected light curve in 3–20 keV, is displayed in this figure. A strong pulsation peak at $\sim 9.7^{+0.03}_{0.03}$ mHz is observed in the PDS. Harmonics of the pulse peak at $0.2^{+0.01}_{-0.01}$ mHz and $0.3^{+0.01}_{-0.01}$ mHz are also observed in the same PDS.

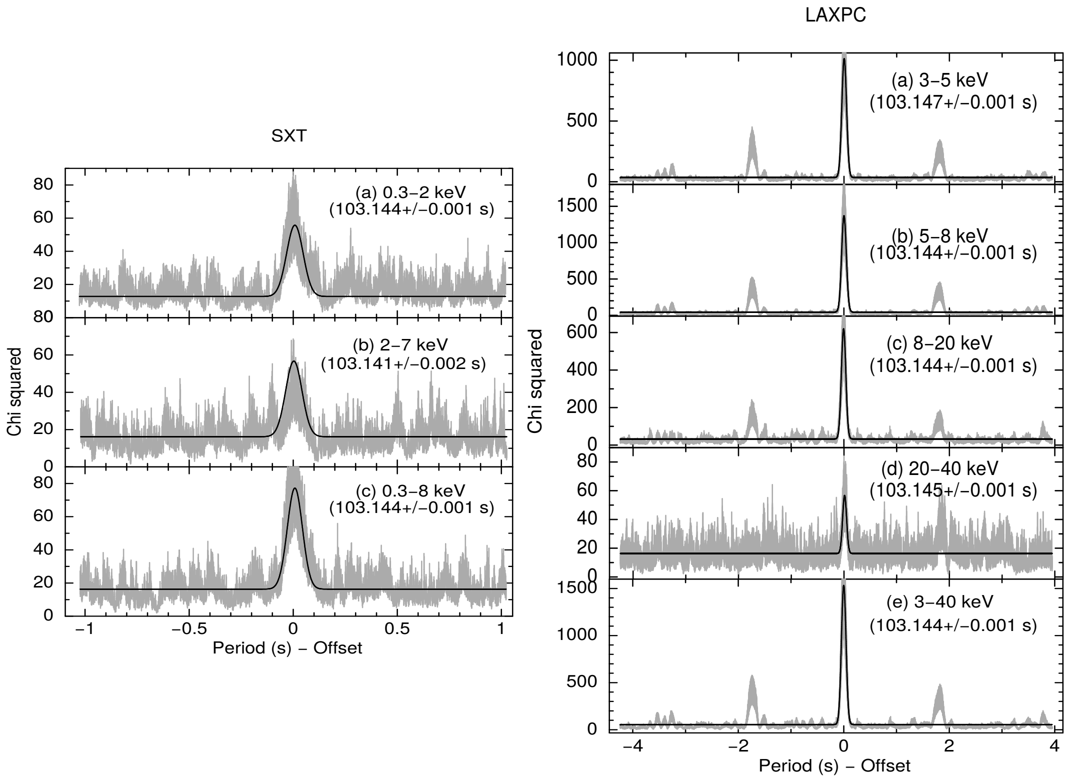

Fig. 4 The best fit pulse period of the pulsar 3A 0726–260 estimated using ftool "efsearch" from SXT and combined LAXPC 10 and LAXPC 20 light curves. The left panel features the best pulsation period estimated from the source in different energy intervals, considering a 2.3775 s binned barycenter corrected SXT light curve. The right panel showcases the best pulsation period derived from barycenter corrected 1 s binned LAXPC light curves.

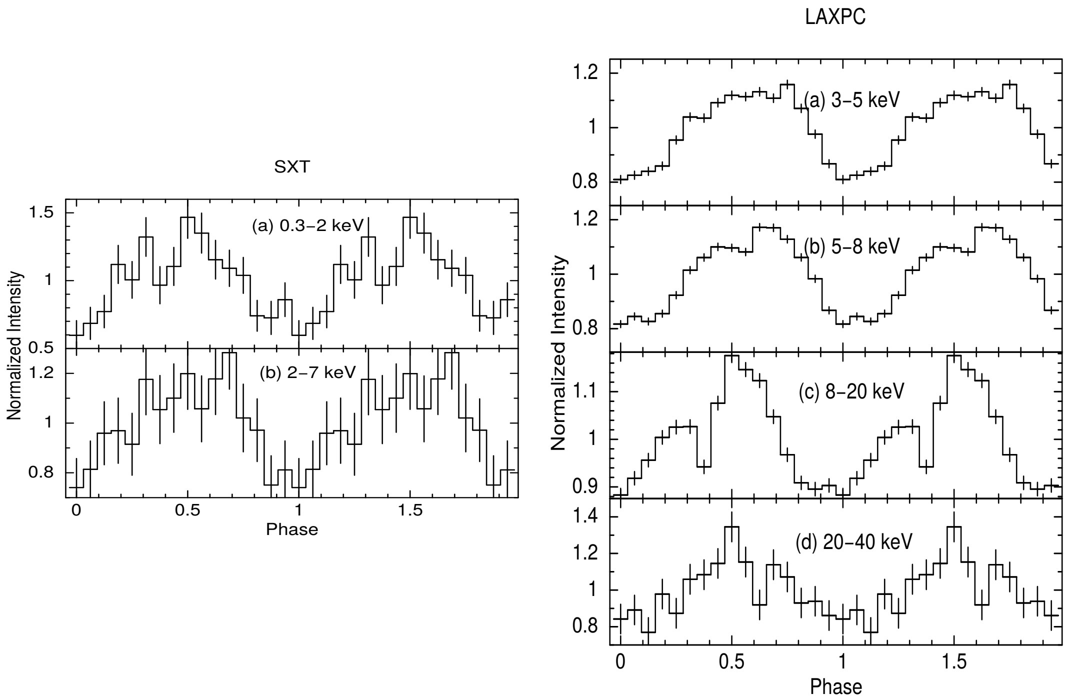

Fig. 5 The energy evolution of pulse profile generated using ftool "efold" is displayed in this figure. Left panels shows pulse profile in (a) 0.3–2 keV and (b) 2–7 keV generated from 2.3775 s binned SXT light curves. Also, the right panel presents pulse profiles generated from LAXPC light curves in (a) 3–5 keV, (b) 5–8 keV, (c) 8–20 keV and (d) 20–40 keV. These single and double peaked pulse profiles have been generated by folding with their best fit pulse periods and 16 phase bins/period.

energy, E_c is the cut off energy in keV and E_f is the e-folding energy in keV.

Table 2 Details of Best Fit Spectral Parameters of Combined SXT (0.4–7 keV), LAXPC 10 and LAXPC 20 (4.0–20 keV) Energy Spectra

Model	Parameter	Value
	Combined SXT and LAXPC	
TBabs	nH (10^{22} cm^{-2})	0.75 (Fixed)
Powerlaw	PhoIndex (Γ)	$1.7^{+0.03}_{-0.03}$
Highecut	cutoffE (keV)	$12.9^{+0.7}_{-0.7}$
	foldE (keV)	$10.9^{+2.4}_{-2.0}$
Gaussian	LineE (keV)	$6.3^{+0.3}_{-0.4}$
	Sigma (keV)	$1.1^{+0.4}_{-0.4}$
	Norm ($\times 10^{-4}$)	$1.9^{+0.8}_{-0.7}$
Constant	SXT	1.0 (Fixed)
	LAXPC 10	0.74±0.04
	LAXPC 20	0.84±0.04
Reduced χ^2 (dof)	Without highecut & gaussian	2.8 (171)
	Without gaussian	1.6 (169)
Reduced χ^2 (dof)	Best fit	1.3 (166)
Flux (0.4–20 keV)	ergs cm^{-2} s^{-1} ($\times 10^{-11}$)	$8.6^{+0.3}_{-0.3}$
Flux (0.4–7 keV)	ergs cm^{-2} s^{-1} ($\times 10^{-11}$)	$6.6^{+0.3}_{-0.2}$
Flux (4–20 keV)	ergs cm^{-2} s^{-1} ($\times 10^{-11}$)	$3.9^{+0.3}_{-0.2}$

Further, a high energy cutoff (White et al. 1983) model available in XSPEC is added to the absorbed powerlaw (see Equation 1). We obtained a significant improvement in the fit parameters with χ^2/dof=1.59 (268/169). This model leaves a residual at $\sim$ 6.4 keV. Inclusion of a Gaussian line at 6.3 keV due to iron Kα line significantly improved the fit to χ^2/dof=1.34 (223/166). Total flux and its error have been obtained using "cflux" model in XSPEC. Total flux observed in 0.4–20 keV is inferred as 8.6 $^{+0.3}_{-0.3}$ $\times$ 10^{-11} erg cm^{-2} s^{-1}. The best fit spectral parameters are tabulated in Table 2. Figure 6 depicts the combined SXT and LAXPC unfolded spectrum, and the solid line represents the combined best fit model.

4 RESULTS AND DISCUSSION

The spectral and timing characteristics of the Be/X-ray binary pulsar 3A 0726–260 have been determined from AstroSat, SXT and LAXPC data from 2016 May 6–7 (MJD 57514.83). The observations below 2 keV from SXT are reported for the first time. Steiner et al. (1984) obtained the first X-ray light curve using the Sky Survey Instrument (SSI) on the Ariel V satellite. Corbet & Peele (1997) discovered that the X-ray source in 3A 0726–260 was a pulsar with a spin period of 103.2±0.2 s. The AstroSat observations 20 years later give a spin period of 103.144±0.001 s, indicating that if at all, there has been only a marginal change in the spin period. Corbet & Peele (1997) did not find any clear periodicity in the 20–40 keV PCA light curve. However, due to the higher effective area of LAXPC detectors in the 20–40 keV band (Agrawal 2006), we could

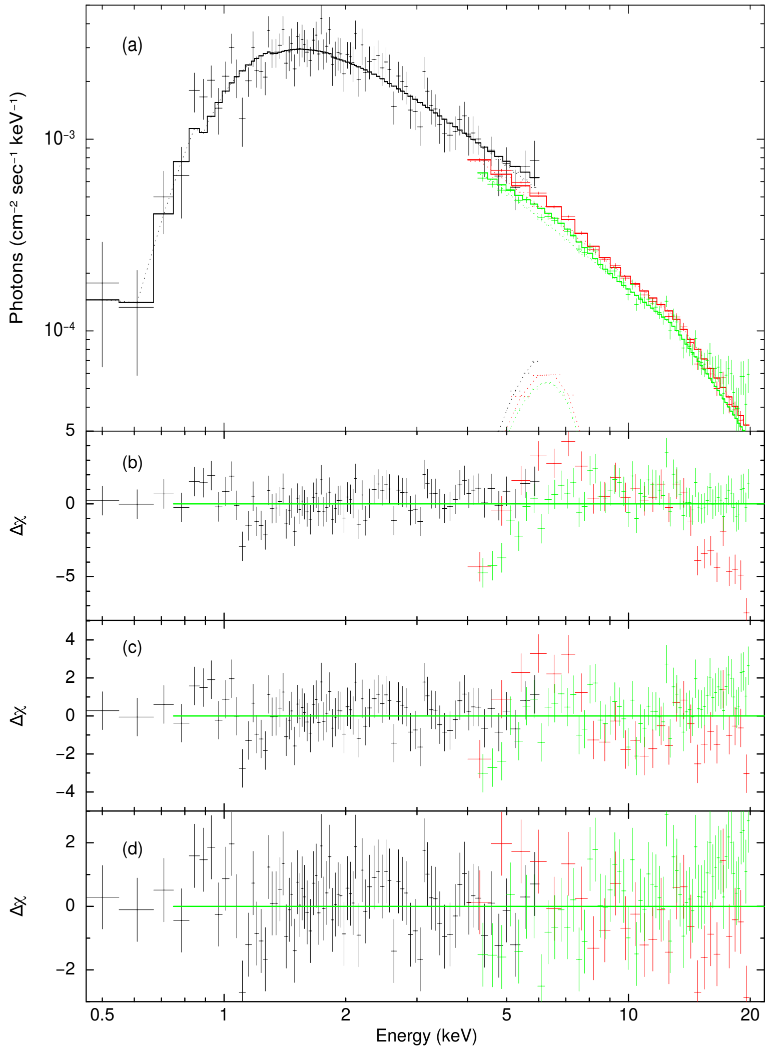

Fig. 6 Panel (a) above displays the unfolded combined energy spectrum. The SXT (0.4–7 keV) derived spectrum is signified in black, and the spectra from LAXPC 10 and 20 (4–20 keV) are marked in green and red, respectively. The best fit models is plotted with a solid line. Panel (b) shows the residuals for the absorbed powerlaw (TBabs*powerlaw) model. Panel (c) presents the residuals after adding the highecut model inbuilt in XSPEC. Panel (d) showcases the residuals after adding the Gaussian line due to the Fe Kα line at $6.3^{+0.3}_{-0.4}$ keV.

detect weak pulsations in the LAXPC data for the first time from the source in the 20–40 keV range. Due to large errors in the 1996 RXTE measurement, it is difficult to derive the rate of variation in the spin period. A crude estimate of the spin-up rate can be made from the two measurements spaced 20 years apart, which gives 8.9×10^{-11} s s^{-1}, and it can be treated as an upper limit. It may be noted from the MAXI light curve that despite being a Be binary, there is no indication of any major outburst in 3A 0726–260 over almost 10 years. This suggests that this pulsar is accreting at almost a steady accretion rate with no indication of any instability leading to a spike in the accretion rate and occurrence of any outburst. The X-ray pulse profile exhibits a single peak structure up to 5 keV. In the pulse profiles above 5 keV, there is a hint of a change from a single peaked profile to a double peak structure. Above 8 keV, appearance of the double peak in the profile is unmistakable, as seen in Figure 5. We observed from Figure 5 that in the double peak pulse profile above eight keV, the first peak is less prominent compared to the second peak whereas, above 20 keV, the first peak becomes stronger compared to the second peak. The estimated values of the pulse fraction in different energy bands are presented in Table 1. The change in the pulse profile from a single peak to a weak double peaked structure may be explained by intrinsic change occurring in the beaming pattern from a pencil beam to a fan beam which results in the beam moving out of our line of sight as observed from the X-ray binary pulsar LMC X-4 (Hung et al. 2010). The change in the pulse profile can also be attributed to a transition in accretion pattern from a smooth accretion stream at low energies to several narrow accretion streams at high energy that are phase-locked with the neutron star as observed from EXO 2030+375 (Naik & Jaisawal 2015). In this work, we deduce the X-ray spectrum in 0.4-20 keV using combined SXT and LAXPC data. The source flux during the AstroSat observation in 2–20 keV is estimated as $5.7\ ^{+0.3}_{-0.3} \times 10^{-11}$ erg cm^{-2} s^{-1}. This is in agreement with the flux value 6.9×10^{-11} erg cm^{-2} s^{-1} reported by Corbet & Peele (1997), from RXTE/PCA observation of the source on 1997 June 7 (MJD 50606). The power-law spectrum is steeper with photon index Γ=$1.7^{+0.03}_{-0.03}$ compared to the RXTE/PCA value. In the spectrum, there is no indication of the presence of any cyclotron line feature in the spectrum. Corbet & Peele (1997) reported a hint of an iron line at $\sim$ 6.6 keV and width $\sim$ 150 eV. In this work, we clearly detect the presence of a broad $1.06^{+0.4}_{-0.4}$ keV iron Kα line at $\sim$ 6.3 keV in the combined SXT and LAXPC spectrum. The broad iron line feature may be due to the presence of two lines at $\sim$ 6.4 keV and $\sim$ 6.6 keV, which could not be clearly resolved by LAXPC detectors. Hopefully, more spectral studies in the future will resolve this ambiguity.

Acknowledgements We are thankful to the reviewer for the constructive comments, which improved the manuscript. This publication uses the data from the AstroSat mission of the Indian Space Research Organisation (ISRO), archived at the Indian Space Science Data Centre (ISSDC). This work has used the AstroSat data from the Large Area X-ray Proportional Counter (LAXPC) detectors developed at TIFR, Mumbai. We would like to thank the LAXPC team for verifying and releasing the data via the ISSDC data archive and providing the necessary software tools. This work has used data from the Soft X-ray Telescope (SXT) developed at TIFR, Mumbai, and the SXT POC at TIFR is thanked for verifying and releasing the data via the ISSDC data archive and providing the necessary software tools. This paper makes use of our proposed data from the AstroSat mission of the Indian Space Research Organisation (ISRO), archived at the Indian Space Science Data Centre (ISSDC). JR would like to thank ISRO for providing funding support. JR would like to thank IUCAA for providing facilities. B. Singari contributed to the work during his two month visit at UM-DAE CEBS as an SARP student. JR thanks Prof. A. R. Rao for valuable suggestions and discussions. This research has made use of softwares obtained through the HEASARC Online Service, provided by NASA/GSFC, in support of NASA High Energy Astrophysics Programs. This research has made use of MAXI data provided by RIKEN, JAXA and the MAXI team.

References

Agrawal, P. C. 2006, Advances in Space Research, 38, 2989
Agrawal, P. C., Yadav, J. S., Antia, H. M., et al. 2017, Journal of Astrophysics and Astronomy, 38, 30
Antia, H. M., Yadav, J. S., Agrawal, P. C., et al. 2017, ApJS, 231, 10
Arnaud, K. A. 1996, XSPEC: The First Ten Years, in ASPC Series, 101, Astronomical Data Analysis Software and Systems V, eds. G. H. Jacoby & J. Barnes, 17
Corbet, R. H. D., Coley, J. B., & Krimm, H. A. 2016, The Astronomer's Telegram, 9823, 1
Corbet, R. H. D., & Mason, K. O. 1984, A&A, 131, 385
Corbet, R. H. D., & Peele, A. G. 1997, ApJL, 489, L83
Forman, W., Jones, C., Cominsky, L., et al. 1978, ApJS, 38, 357
Hung, L.-W., Hickox, R. C., Boroson, B. S., & Vrtilek, S. D. 2010, ApJ, 720, 1202
Naik, S., & Jaisawal, G. K. 2015, RAA (Research in Astronomy and Astrophysics), 15, 537
Nakajima, M., Mihara, T., Iwakiri, W., et al. 2016, The Astronomer's Telegram, 9820, 1
Negueruela, I., Roche, P., Buckley, D. A. H., et al. 1996, A&A, 315, 160
Nespoli, E., & Reig, P. 2011, A&A, 526, A7
Roy, J., Agrawal, P. C., Dedhia, D. K., et al. 2016, Experimental Astronomy, 42, 249
Singh, K. P., Tandon, S. N., Agrawal, P. C., et al. 2014, in SPIE Conference Series, 9144, 91441S
Singh, K. P., Stewart, G. C., Chandra, S., et al. 2016, in SPIE Conference Series, 9905, 99051E
Singh, K. P., Stewart, G. C., Westergaard, N. J., et al. 2017, Journal of Astrophysics and Astronomy, 38, 29
Steiner, J. E., Ferrara, A., Garcia, M., et al. 1984, ApJ, 280, 688
Stella, L., & Angelini, L. 1992, in Data Analysis in Astronomy, 59
Warwick, R. S., Marshall, N., Fraser, G. W., et al. 1981, MNRAS, 197, 865
White, N. E., Swank, J. H., & Holt, S. S. 1983, ApJ, 270, 711
Wilms, J., Allen, A., & McCray, R. 2000, ApJ, 542, 914
Wood, K. S., Meekins, J. F., Yentis, D. J., et al. 1984, ApJS, 56, 507
Yadav, J. S., Agrawal, P. C., Antia, H. M., et al. 2016, in SPIE Conference Series, 9905, 99051D